Journal of Chromatography A, 1226 (2012) 103–109

Contents lists available at ScienceDirect

Journal of Chromatography A

journal homepage: www.elsevier.com/locate/chroma

Stationary phase selection and comprehensive two-dimensional gas chromatographic analysis of trace biodiesel in petroleum-based fuel

John V. Seeley[a,*], Carly T. Bates[a], James D. McCurry[b], Stacy K. Seeley[c]

[a] Oakland University, Department of Chemistry, Rochester, MI 48309, USA
[b] Agilent Technologies, Inc., Wilmington, DE 19808, USA
[c] Kettering University, Department of Chemistry & Biochemistry, Flint, MI 48504, USA

ARTICLE INFO

Article history:
Available online 30 July 2011

Keywords:
Comprehensive two-dimensional chromatography
Jet fuel
Biodiesel
Gas chromatography
Retention time prediction
Solvation parameter model

ABSTRACT

The GC × GC solvation parameter model has been used to identify effective stationary phases for the separation of fatty acid methyl esters (FAMEs) from petroleum hydrocarbons. This simple mathematical model was used to screen the 1225 different combinations of 50 stationary phases. The most promising pairs combined a poly(methyltrifluoropropylsiloxane) stationary phase with a poly(dimethyldiphenylsiloxane) stationary phase. The theoretical results were experimentally tested by equipping a GC × GC instrument with a DB-210 primary stationary phase and an HP-50+ secondary stationary phase. This instrument was used to analyze trace levels of FAMEs in kerosene. The FAMEs were fully separated from the petroleum hydrocarbons on the secondary dimension of the 2-D chromatogram. The resulting GC × GC method was shown to be capable of accurately quantifying FAME levels as low as 2 ppm (w/w). These results demonstrate the utility of the solvation parameter model for identifying optimal stationary phases for high resolution GC × GC separations. Furthermore, this work presents an effective method for determining the level of biodiesel contamination in aviation fuel and other petroleum-based fuels.

1. Introduction

There is growing concern that biodiesel residue in pipelines can contaminate aviation fuel. The pipelines and tanks used to distribute jet fuel are also used in the distribution of other fuels including biodiesel blends. According to the United States Federal Aviation Administration (FAA), the fatty acid methyl esters (FAMEs) in biodiesel can adhere to the internal metal surfaces of the pipelines and tanks [1]. The FAME residue can then contaminate other fuels that subsequently use these distribution vessels. At high concentrations, FAMEs threaten the stability of the aviation fuel and may ultimately lead to gelling and/or coke deposits in the fuel system. These conditions can lead to engine failure. The FAA currently specifies that jet fuel containing FAME levels above 30 ppm should not be used [1]. Unfortunately, measuring low levels of FAMES with gas chromatography is difficult due to the thousands of hydrocarbons found in aviation fuel.

Multiple chromatographic methods have been used to characterize blends of biodiesel and petroleum-based fuels [2] including liquid chromatography (LC) [3,4], gas chromatography (GC) [5], and gas chromatography–mass spectrometry (GC–MS) [6–8]. Comprehensive two-dimensional gas chromatography (GC × GC) has also been proven to be effective at characterizing biodiesel blends. Seeley et al. [9] used a valve-based GC × GC instrument to characterize biodiesel blends with FAME concentrations ranging from 1% to 20% (v/v). They employed a primary column with a 5% diphenyl 95% dimethyl polysiloxane stationary phase and a secondary column with a polyethylene glycol stationary phase. This stationary phase combination generated FAME secondary retention times that were greater than those of the highly concentrated alkanes in the petroleum diesel. However, the FAMEs occupied a region of the 2-D chromatogram that was also occupied by the monoaromatic hydrocarbons. Fortunately, the co-eluting monoaromatics were present in low levels and spread throughout the chromatographic region. This led to large, sharp FAME peaks that towered above a low intensity continuum of monoaromatic peaks. Thus, the area of the FAME peaks could be accurately determined by treating the monoaromatic peaks as a locally elevated baseline.

Adam et al. [10] also used a thermal modulation GC × GC instrument to characterize the level of FAMEs in biodiesel blends. They tested the resolving power of combinations of seven different stationary phases. They examined poly(dimethylsiloxane), cyanopropyl-substituted polysiloxanes, phenyl-substituted polysiloxanes, and polyethylene glycol stationary phases. They found that the best resolution of the individual FAMEs was achieved with a polyethylene glycol primary column and a

* Corresponding author. Tel.: +1 248 370 2329; fax: +1 248 370 2321.
E-mail address: seeley@oakland.edu (J.V. Seeley).

0021-9673/$ – see front matter © 2011 Elsevier B.V. All rights reserved.
doi:10.1016/j.chroma.2011.07.075

poly(dimethylsiloxane) secondary column, but the FAMEs still eluted in the monoaromatic region of the 2-D chromatogram. However, when Adam et al. analyzed biodiesel blends containing 5% (v/v) FAMEs, the results were still highly accurate due to the much greater concentrations of FAMEs as compared to the co-eluting monoaromatic hydrocarbons.

Tiyapongpattana et al. [11] analyzed 5% (v/v) blends of biodiesel using thermal modulation GC × GC with a 5% diphenyl 95% dimethyl polysiloxane × polyethylene glycol column combination. They analyzed mixtures of FAMEs generated from a wide range of sources including vegetable oils, animal fats, and waste cooking oils. This study also demonstrated that the 5% biodiesel blends could be accurately quantified. Once again, the FAMEs co-eluted with low intensity monoaromatic hydrocarbons.

Most recently, Pierce and Schale [12] accurately characterized biodiesel blends ranging from 5% to 20% (v/v) using a thermal modulation GC × GC–MS instrument with chemometric data analysis. They employed a primary column with a 5% diphenyl 95% dimethyl polysiloxane stationary phase and a secondary column with a poly(methyltrifluorylpropylsiloxane) stationary phase. This column combination caused the FAMEs to have substantially higher secondary retention times than saturated hydrocarbons but the FAMEs still overlapped with the polycyclic aromatic hydrocarbons.

The previously described GC × GC methods did not fully resolve the FAMEs from the petroleum hydrocarbons. However, they were still effective for analyzing biodiesel/petroleum blends due to the high FAME concentrations. These GC × GC methods would presumably be less effective if the FAME levels were comparable to the co-eluting hydrocarbons. Thus, these methods would most likely be ineffective at quantifying ppm-levels of FAMEs in diesel fuel (i.e., FAME levels that are 10,000 times less than commercial blends).

The ideal GC × GC method would fully resolve FAMEs from the petroleum hydrocarbons. Such a method would allow a wide range of FAME concentrations to be determined accurately in blends with any petroleum-based fuel. One way to achieve this goal is to find a pair of stationary phases where FAMEs are fully separated from the hydrocarbon classes (i.e., acyclic alkanes, cyclic alkanes, monoaromatics, polycyclic aromatics, alkenes, etc.) along the secondary dimension.

Seeley et al. [13] recently developed an extension of the Abraham solvation parameter model [14] that predicts the relative retention of compounds in GC × GC chromatograms. The predictions are normally in the form of two-dimensional retention diagrams. Retention diagrams are generated by using the Abraham solvation parameter model to predict the retention indices on both the primary and secondary stationary phases. The primary retention index I_1 is then plotted along the horizontal axis and $1.6^{\Delta I}$ is plotted along the secondary axis where ΔI is the difference between the primary and secondary retention indices (i.e., $\Delta I = I_2 - I_1$). Seeley et al. [13] have shown that peak positions in the retention diagrams are highly correlated with the peak positions in the 2-D chromatograms. The main advantage of this approach is that relative GC × GC retention times can be rapidly predicted for a wide range of stationary phase combinations. Accurate stationary phase descriptors [15] are available for most modern liquid stationary phases and solute descriptors are available for numerous compounds [14,16] or can be estimated [17].

In this article, the GC × GC solvation parameter model is used to screen 50 stationary phases in an effort to find a pair that allows organic esters such as FAMEs to be fully separated from petroleum hydrocarbons. A promising pair of stationary phases is then used to analyze FAME/fuel mixtures. The quantitative accuracy and precision of the resulting methodology is characterized over a wide range of FAME concentrations.

2. Theory and calculations

2.1. The GC × GC solvation parameter model

A detailed account of the GC × GC solvation parameter model has been published [13]. A brief description of the features pertinent to this study follows. The Abraham solvation parameter model has been most frequently used to predict the retention factors of solutes on a single stationary phase [15]. The fundamental equation for these predictions is

$$\log \quad k = lL + sS + eE + aA + c \tag{1}$$

where k is the retention factor; l, s, e, a, and c are stationary phase descriptors; and L, S, E, and A are solute descriptors. The solute descriptors have been interpreted [15] as follows: L represents the ability of the solute to engage in dispersive interactions, S represents a combination of the dipolarity and polarizability of the solute, E represents the ability of the solute to establish induced-dipole interactions through its π electrons and lone pair electrons, and A represents the hydrogen bond acidity of the solute. The stationary phase descriptors represent the weight placed on each of the solute characteristics with the exception of the c term that is largely determined by the phase ratio of the column. For example, non-polar columns interact primarily through dispersion forces so they heavily weight the L factor (i.e., they have large values of l) and place a smaller weight on the polar descriptors (i.e., they have much smaller values of s, e, and a). In contrast, polar columns have slightly smaller values of l and much larger values of one or more of the polar weighting factors s, e, and a.

The GC × GC adaptation of the solvation parameter model first predicts the retention index of each solute on the primary stationary phase and the secondary stationary phase. Retention indices are calculated by algebraically transforming Eq. (1) to the following

$$I = L' + s'S' + e'E' + a'A' \tag{2}$$

where I is a retention index that increases by approximately 1 when a methylene group is added to a homologous compound (i.e., I is essentially a Kovats retention index divided by 100). The descriptors designated with "prime" symbols in Eq. (2) are directly related to the original solvation parameter model descriptors of Eq. (1) by the following relationships

$$L' = \left(\frac{L - 0.244}{0.493}\right) \tag{3}$$

$$S' = \left(\frac{S}{0.493}\right) \tag{4}$$

$$E' = \left(\frac{E}{0.493}\right) \tag{5}$$

$$A' = \left(\frac{A}{0.493}\right) \tag{6}$$

$$s' = \left(\frac{s}{l}\right) \tag{7}$$

$$e' = \left(\frac{e}{l}\right) \tag{8}$$

$$a' = \left(\frac{a}{l}\right) \tag{9}$$

The values of the original solute descriptors L, S, E, and A are by definition temperature invariant [15]. Thus, the values of L', S', E', and A' are also temperature invariant. In contrast, the stationary phase descriptors l, s, e, and a are temperature dependent. For simplicity, the temperature averaged values of s', e', and a' are used in the GC × GC solvation parameter model.

The retention indices are used to predict the retention order. The order along the primary retention axis is modeled by the predicted primary retention index

$$I_1 = L' + s_1'S' + e_1'E' + a_1'A' \quad (10)$$

where s_1', e_1', and a_1' are the polarity descriptors for the primary stationary phase.

The retention order along the secondary axis is modeled by a factor of 1.6 raised to the difference between the secondary and primary retention indices ΔI. Thus, the predicted secondary retention position increases exponentially with ΔI. The retention index difference is determined from the following equation:

$$\Delta I = I_2 - I_1 = (L' + s_2'S' + e_2'E' + a_2'A') - (L' + s_1'S' + e_1'E' + a_1'A') \quad (11)$$

where s_2', e_2', and a_2' are the polarity descriptors for the secondary stationary phase.

The values of L' cancel and the value of ΔI is given by

$$\Delta I = (s_2' - s_1')S' + (e_2' - e_1')E' + (a_2' - a_1')A' \quad (12)$$

Thus, the value of ΔI, and hence the predicted secondary retention order, is determined by the difference in the polarity descriptors of the primary and secondary stationary phases and the polar descriptors of the solutes.

2.2. Applying the GC × GC solvation parameter model to FAMEs and petroleum hydrocarbons

Under ideal circumstances, the GC × GC solvation parameter model would be used to generate a 2-D retention diagram that predicts the relative position of all of the sample components in a 2-D chromatogram. However, such an approach is not feasible in the case of petroleum-based fuels blended with biodiesel as solute descriptors are only available for a small fraction of the components. A simpler approach for screening stationary phase pairs can be employed if the focus is exclusively shifted to the secondary dimension. This simplifies the analysis because (1) the retention order along the secondary dimension is determined only by the solute and stationary phase polarity descriptors, and (2) the solute polarity descriptors are very similar within members of the same functional class (e.g., many alkyl esters have nearly identical values of S' and E') [16]. Thus, a fairly accurate estimate of the range of polarity descriptors can be obtained by examining several members of each relevant compound class.

The simulations described in this article focus completely on finding a pair of stationary phases that can separate alkyl esters including FAMEs from petroleum hydrocarbons on the secondary dimension. The first step is to use Eqs. (4) and (5) to calculate the solute polarity descriptors for the hydrocarbons and alkyl esters present in the Poole data sets [15,16,18,19]. The process is simplified by the fact that alkyl esters and hydrocarbons do not possess hydrogen bond acidity (i.e., $A = 0$ for each compound in these classes) due to their lack of electropositive hydrogen atoms. Thus, the values of A' are all equal to zero. The values of S' and E' were calculated from the Poole data and are listed in Table 1. The solute set includes 32 hydrocarbons and 8 alkyl esters. A plot of the S' and E' values of the compounds is shown in Fig. 1. This plot clearly shows the strong linear correlation of the S' and E' parameters for the hydrocarbons. Increasing the degree of unsaturation and/or cyclization of the hydrocarbons causes their S' and E' values to both increase. The line in Fig. 1 represents the best fit to the hydrocarbon data and has an equation of $E' = 1.42\ S'$. The data also show that the alkyl esters have S' values similar to those of the monoaromatic hydrocarbons, but much smaller E' values. Thus, the alkyl esters occupy a region of the polarity descriptor space that is fully separated from the hydrocarbon band.

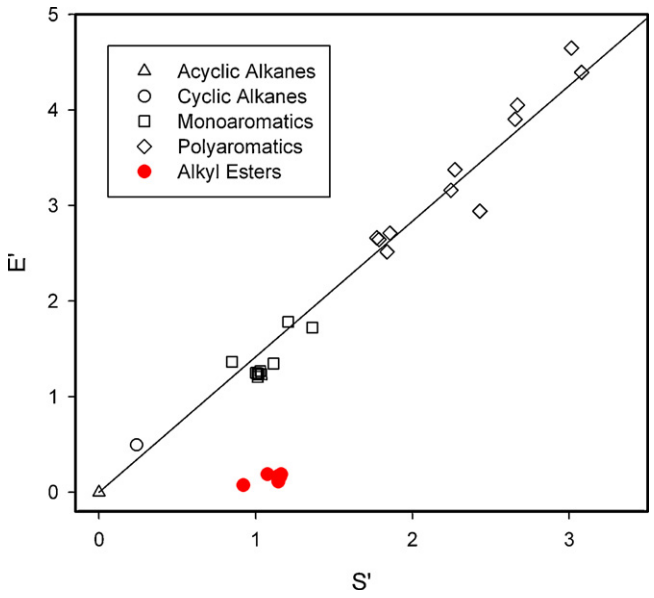

Fig. 1. Polarity descriptors for the hydrocarbons and alkyl esters calculated from the Poole data set.

The retention order along the secondary dimension can be predicted using Eq. (12) to calculate ΔI. The GC × GC solvation parameter model assumes that the retention along the secondary dimension is linearly related to $1.6^{\Delta I}$. The function $1.6^{\Delta I}$ monotonically increases with ΔI. Thus, the model predicts that the hydrocarbons will be separated from the alkyl esters if the ΔI values of the alkyl esters do not overlap with the ΔI values of the hydrocarbons. Because hydrocarbons and alkyl esters all have A' values equal to zero, Eq. (12) simplifies to

$$\Delta I = (s_2' - s_1')S' + (e_2' - e_1')E' = \Delta s'S' + \Delta e'E' \quad (13)$$

Eq. (13) shows that the values of ΔI for each compound are calculated by multiplying the S' and E' solute descriptors by the differences in the s' and e' descriptors of the primary and secondary phases. Table 2 shows the five stationary phases that were initially examined in this study along with their values of s' and e'. These stationary phases were selected because (1) they are similar to the stationary phases used in previous GC × GC separations of biodiesel/petroleum blends, and (2) they represent a wide range of stationary phase selectivities. The tabulated values of s' and e' represent the temperature averaged values of s' and e' from 60 to 140 °C (i.e., the full temperature range reported by Poole and Poole [15]).

These five stationary phases can be combined to generate 10 different stationary phase pairs. The pairs along with their values of $\Delta s'$ and $\Delta e'$ are shown in Table 3. Changing the stationary phase order for a given pair changes the sign of the $\Delta s'$ and $\Delta e'$ terms and hence changes only the sign of the calculated values of ΔI. These simulations are strictly looking for overlap in the ΔI values of the alkyl esters with the ΔI values of the hydrocarbons. Changing the sign of all the ΔI values does not change the degree of overlap of the ΔI values. Thus, calculating the ΔI values for a stationary phase pair provides information for both stationary phase orders.

2.3. Secondary retention order predictions and comparison with prior results

The values of ΔI were calculated using Eq. (13) for each compound in Table 1 with each stationary phase pair in Table 3. The values of ΔI are shown in Fig. 2 for the 10 possible stationary phase pairs. The prediction for DB-1 × DB-WAXetr is shown

Table 1
Calculated solute descriptors.

	S'	E'		S'	E'
Acyclic alkanes			*Polyaromatic hydrocarbons*		
Octane	0.00	0.00	Naphthalene	1.84	2.52
Nonane	0.00	0.00	1-Methylnaphthalene	1.86	2.71
Decane	0.00	0.00	2-Methylnaphthalene	1.79	2.65
Undecane	0.00	0.00	Fluorene	2.27	3.38
Dodecane	0.00	0.00	Acenaphthylene	2.25	3.16
Tridecane	0.00	0.00	Phenanthrene	2.67	4.05
Tetradecane	0.00	0.00	Anthracene	2.66	3.90
Hexadecane	0.00	0.00	Fluoranthene	3.01	4.65
Octadecane	0.00	0.00	Pyrene	3.08	4.39
			Biphenyl	1.77	2.66
Cyclic alkanes			trans-Stilbene	2.43	2.94
Methylcyclohexane	0.24	0.49			
Monoaromatics hydrocarbons			*Alkyl esters*		
Benzene	1.04	1.23	Propyl acetate	1.16	0.19
Toluene	1.01	1.23	n-Butyl acetate	1.16	0.16
Ethylbenzene	1.01	1.24	Ethyl propionate	1.08	0.19
n-Propylbenzene	1.02	1.24	Ethyl 2-methylbutyrate	0.92	0.07
n-Butylbenzene	1.01	1.21	Methyl hexanoate	1.14	0.17
m-Xylene	1.03	1.27	Methyl octanoate	1.14	0.14
p-Xylene	1.00	1.25	Methyl nonanoate	1.14	0.11
o-Xylene	1.11	1.34	Methyl decanoate	1.14	0.12
Styrene	1.36	1.72			
Phenylcyclohexane	1.21	1.78			
1,3,5-Triethylbenzene	0.85	1.36			

Table 2
Descriptors for five stationary phases.

Stationary phase	Composition	s'	e'
DB-1	Poly(dimethylsiloxane)	0.412	−0.030
DB-1701	Poly(cyanopropylphenyldimethylsiloxane)14% cyanopropylphenylsiloxane	1.350	−0.229
HP-50+	Poly(dimethyldiphenylsiloxane) 50% diphenylsiloxane	1.402	0.196
DB-WAXetr	Poly(ethylene glycol)	2.841	0.425
DB-210	Poly(methyltrifluoropropylsiloxane)	2.966	−0.990

at the top of Fig. 2. The hydrocarbon ΔI values increase in the order of acyclic alkanes < cyclic alkanes < monoaromatic hydrocarbons < polyaromatic hydrocarbons. This retention order is in agreement with the experimental observations of GC × GC separations of petroleum fuels using a nonpolar primary stationary phase and a polyethylene glycol secondary stationary phase [9,11]. The values of ΔI for the alkyl esters are shown to overlap with the monoaromatics for the DB-1 × DB-WAXetr configuration. Thus, the simulation predicts that alkyl esters would overlap with monoaromatics along the secondary axis. This is in agreement with the 2-D chromatograms reported by Seeley et al. [9] for an HP-5 × DB-WAX column set and Tiyapongpattana et al. [11] for a BPX-5 × BP20 column set.

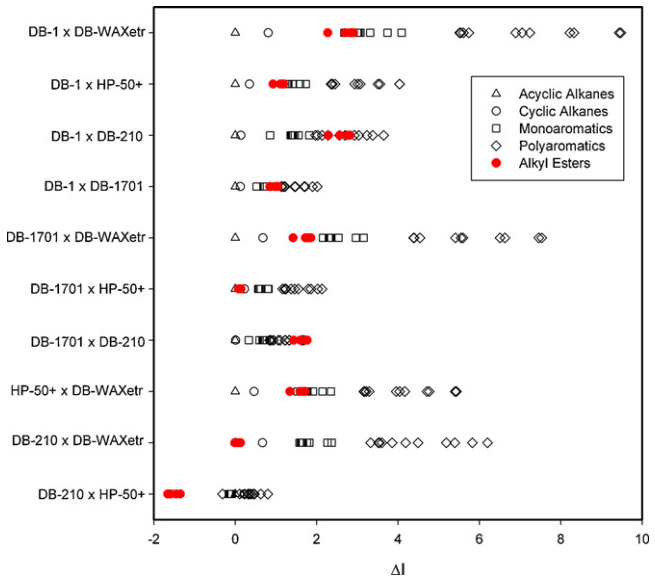

Fig. 2. ΔI values calculated for 10 different stationary phase combinations.

The calculated order of the ΔI values is simply reversed for a DB-WAXetr × DB-1. Thus, the secondary retention order is predicted to be polyaromatic hydrocarbons < monoaromatic hydrocarbons < cyclic alkanes < acyclic alkanes and the alkyl esters are still predicted to co-elute with the monoaromatic hydrocarbons. This is in agreement with the chromatograms published by Adam et al. [10] for a Solgel Wax × DB-1 column set.

The prediction for DB-1 × HP-50+ is shown in Fig. 2. The ΔI values show the same order as the DB-1 × DB-WAXetr pair, but the range of ΔI values is smaller. This is due to the smaller polarity difference between DB-1 and HP-50+. The overlap of the alkyl esters with the hydrocarbons is consistent with the investigation of Adam et al. [10] who found that the FAMEs co-eluted with both cyclic alkanes and monoaromatic hydrocarbons when a PONA × BPX-50 stationary phase combination was employed.

The simulation for DB-1 × DB-210 is also shown in Fig. 2. The model predicts that alkyl esters will have secondary retention times that are overlapping with the polyaromatic hydrocarbons. This prediction matches the experimental results obtained by Pierce and Schale [12] using RTX-5ms × RTX-200ms.

The next six stationary phase pairs (i.e., DB-1 × DB-1701, DB-1701 × DB-WAXetr, DB-1701 × HP-50+, DB-1701 × DB-210, HP-50+ × DB-WAXetr, and DB-210 × DB-WAXetr) all place the alkyl esters within the range of hydrocarbon ΔI values. Experimental data is not available for all of these combinations; however,

Table 3
Polarity differences of stationary phase pairs from the initial set.

Stationary phase combination	$\Delta s'$	$\Delta e'$
DB-1 × DB-WAXetr	2.429	0.455
DB-1 × HP-50+	0.990	0.226
DB-1 × DB-210	2.554	−0.96
DB-1 × DB-1701	0.938	−0.199
DB-1701 × DB-WAXetr	1.491	0.654
DB-1701 × HP-50+	0.052	0.425
DB-1701 × DB-210	1.616	−0.761
HP-50+ × DB-WAXetr	1.439	0.229
DB- WAXetr × DB-210	0.125	−1.415
DB-210 × HP-50+	−1.564	1.186

Adam et al. [10] obtained data for Solgel Wax × DB-1701 and Solgel Wax × BPX-50. They reported that both of these pairs caused the FAMEs to co-elute with the monoaromatic hydrocarbons. The simulated column sets of DB-1701 × DB-WAXetr and HP-50+ × DB-WAXetr (see Fig. 2) are most similar to Solgel Wax × DB-1701 and Solgel Wax × BPX-50, respectively. The calculations correctly predict that the alkyl esters will elute within the secondary retention range of the hydrocarbons closest to the monoaromatic hydrocarbons.

Of the 10 column combinations considered in Fig. 2, the DB-210 × HP-50+ pair is predicted to generate the best separation of the alkyl esters from the hydrocarbons because it successfully exploits the polarity differences between the alkyl esters and the hydrocarbons. The alkyl esters have much larger S' values than E' values. Thus, the $\Delta s'$ value of −1.564 for the DB-210 × HP-50+ combination (see Table 3) causes the ΔI values of alkyl esters to be negative. In contrast, the hydrocarbons have E' and S' values that are equal to 0 for n-alkanes or E' values that are approximately 40% larger than their S' values for cyclic alkanes and aromatic hydrocarbons. The $\Delta s'$ value of −1.564 and the $\Delta e'$ value of 1.186 cause the hydrocarbons to have ΔI values clustered between 0 and 1.

2.4. Expanding the search for optimal stationary phase pairs

Poole and Poole [15] also generated accurate descriptors for 50 GC stationary phases (including the 5 stationary phases shown in Table 2). Their data set included polar siloxanes with high levels of cyanopropyl substitution (e.g., HP-88 and BPX-90) but did not include ionic liquid stationary phases. Simulations similar to those shown in Fig. 2 were performed for the 1225 possible combinations of the 50 stationary phases. An in-house written computer program was used to perform this analysis. Column combinations were evaluated by examining the ΔI values calculated for the hydrocarbons and the alkyl esters. The most promising column combinations were selected based on the following criteria: (1) no overlap between the hydrocarbon ΔI values and the alkyl ester ΔI values and (2) a greater than 0.80 separation between the hydrocarbons and alkyl esters along the ΔI axis. Of the 1225 column combinations analyzed, only 7 met these criteria (see Table 4). The distribution of ΔI values for each of these pairs is similar to that predicted for the DB-210 × HP-50+ pair shown in Fig. 2. In each of the 7 promising pairs, one stationary phase is a trifluoropropyl substituted siloxane (DB-210 or DB-200) and the other stationary phase is a siloxane with high levels of phenyl substitution (Rtx-65, HP-50+, DB-608, DB-17ms, Rtx-50, DB-35, or DB-35ms). Such combinations generate a secondary selectivity where the $\Delta s'$ value is negative and has a large enough magnitude to separate the alkyl esters from the alkanes. Furthermore, these optimal pairs have a $\Delta s'/\Delta e'$ ratio near −1.3. This ratio is particularly well suited for counter balancing the S' and E' values of the hydrocarbons causing them to have ΔI values in the range of 0–1.

Table 4
Polarity differences for optimal stationary phase pairs.

Stationary phase combination	$\Delta s'$	$\Delta e'$	$\Delta s'/\Delta e'$
DB-210 × Rtx-65	−1.383	1.147	−1.206
DB-210 × HP-50+	−1.564	1.186	−1.319
DB-210 × DB-608	−1.543	1.156	−1.335
DB-210 × DB-17ms	−1.547	1.136	−1.362
DB-210 × Rtx-50	−1.458	1.086	−1.343
DB-200 × DB-35	−0.983	0.831	−1.183
DB-200 × DB-35ms	−0.961	0.811	−1.185

Based on the model predictions described above, the DB-210 and HP-50+ stationary phase pair was determined to be a good choice to fully separate FAMEs from petroleum hydrocarbons. However, the solvation parameter model provides little information on the most effective stationary phase order (i.e., DB-210 × HP-50+ as opposed to HP-50+ × DB-210). The previous study of Seeley et al. [13] has shown that the GC × GC solvation parameter model slightly under-predicts the secondary retention of highly cyclized compounds when compared to linear compounds. Thus, it is likely that the polycyclic hydrocarbons in petroleum-based fuels will experience slightly greater secondary retention than predicted from the ΔI plots shown in Fig. 2. The model predicts that a DB-210 × HP-50+ configuration will place the FAMEs beneath the hydrocarbons in the 2-D chromatogram (i.e., the FAMEs will have lower secondary retention than the hydrocarbons). Any additional secondary retention of the highly cyclized hydrocarbons will push them upward along the secondary axis increasing their separation from the FAMEs. In contrast, the model predicts that the reverse configuration (i.e., HP-50+ × DB-210) will place the FAMEs above the hydrocarbons in the 2-D chromatogram. Increased secondary retention for polycyclic hydrocarbons will cause them to be pushed upward toward the FAMEs, thereby decreasing the separation. Therefore, it was predicted that the DB-210 × HP-50+ configuration would be more effective at isolating the FAMEs than the HP-50+ × DB-210 configuration.

3. Materials and methods

The GC × GC system is similar to a previously described apparatus [9]. Briefly, an Agilent Technologies, Inc. (Wilmington, DE, USA) 6890N gas chromatograph was equipped with an Agilent 7683 series injector, electronic pneumatics, and a flame ionization detector (FID). Ultra high purity hydrogen was used as a carrier gas. Samples were injected into a split inlet and operated at a 10:1 or 100:1 split ratio and at 250 °C. Injected components (1.0 μL) were passed through a 30 m × 0.25 mm DB-210 primary column with a 0.50 μm film thickness (poly(methyltrifluoropropylsiloxane), Agilent Technologies, Inc.). The flow in the primary column was 1.0 mL/min. Upon exiting the primary column, the components were modulated with a differential flow fluidic modulator [20] at a period of 1.5 s and an auxiliary flow rate of 15 mL/min. The modulated peaks were passed through a microvolume tee union (VICI, Inc.) that evenly split the flow between two parallel columns: a 5 m × 0.25 mm HP-50+ column with 0.10 μm film thickness (poly(dimethyldiphenylsiloxane) with 50% diphenylsiloxane monomer incorporation, Agilent Technologies, Inc.), and a 5 m × 0.25 mm fused silica capillary that served as a flow restrictor. The oven temperature program was a 40 °C hold for 2.5 min, a ramp to 260 °C at 12 °C/min, followed by a 5 min hold at 260 °C. The secondary column effluent was monitored with an FID (250 °C, 200 Hz sampling).

The detector signal was recorded with Agilent ChemStation software. The resulting 1-dimensional array was converted into 2-dimensional gas chromatograms for visualization using software developed in-house. Quantitation was performed by first inte-

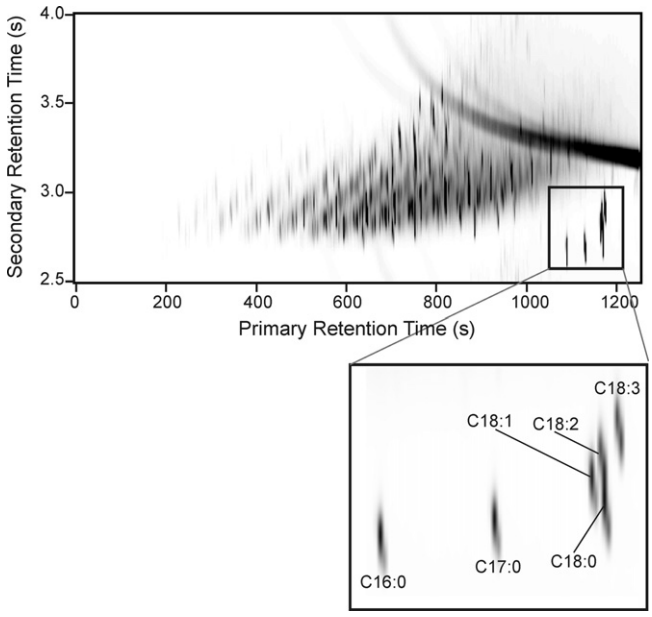

Fig. 3. GC × GC chromatogram of diesel fuel containing 1.0% (w/w) of each of the following fatty acid methyl esters: C16:0, C17:0, C18:0, C18:1, C18:2, and C18:3.

grating the peaks in the original 1-dimensional FID signal array using Agilent ChemStation software. The resulting peak list was imported into custom-written software that employed a peak grouping algorithm and user-defined retention regions to assign each 1-dimensional peak to a specific chemical component. The total area of each group of 1-dimensional peaks was used to quantify the concentration of the corresponding chemical component.

The following pure FAMEs were obtained from Aldrich Chemical: methyl palmitate (C16:0), methyl heptadecanoate (C17:0), methyl stearate (C18:0), methyl oleate (C18:1), methyl linoleate (C18:2), and methyl linolenate (C18:3). An initial set of standard solutions was prepared with 100 ppm of each FAME in dodecane to determine the FAME retention times. A second set of standards was generated to mimic aviation fuel contaminated with varying levels of biodiesel blend. A biodiesel blend containing 1.0% (w/w) of each FAME in diesel was prepared. This solution was then diluted with varying amounts of kerosene to generate individual FAME concentrations of 2, 5, 11, 23, 56, and 98 ppm (w/w). Kerosene was chosen as a substitute for aviation fuel as it was readily available and is known to have a hydrocarbon composition that closely resembles aviation fuel. An actual aviation fuel sample was obtained near the conclusion of these studies (JP8-Jet Fuel, Delek US, Tyler TX, USA). A side-by-side GC × GC comparison using the experimental conditions described above confirmed the high level of similarity between kerosene and aviation fuel. It was concluded that the analyses described below would be as effective for aviation fuel samples as kerosene samples.

4. Results and discussion

4.1. GC × GC separation of a biodiesel blend

Fig. 3 shows the GC × GC chromatogram of a FAME/diesel fuel mixture. Each FAME (C16:0, C17:0, C18:0, C18:1, C18:2, and C18:3) is present at a 1.0% (w/w) concentration. The FAMEs elute in the lower right hand corner of the chromatogram, beneath the wedge-shaped mass of peaks representing the diesel fuel hydrocarbons. The FAMEs are fully resolved from the hydrocarbons. Some diagonal bands can be seen in the hydrocarbon peaks, but there is no clear separation between the different hydrocarbons classes. An additional series of analyses was performed with several sets of standards containing n-alkanes, cyclohexanes, 1-alkenes, and polycyclic aromatic hydrocarbons. From these analyses, it was determined that all hydrocarbon classes have similar secondary retention times, in agreement with the model predictions. The entire separation took approximately 26 min to complete. The DB-210 primary column was observed to have a substantial amount of stationary phase bleed as the temperature approach 260 °C (i.e., the recommended maximum temperature of the stationary phase), as evidenced by the downward sloping band that begins at 700 s and increases in intensity as the primary retention time (and hence the oven temperature) increases.

As predicted by the GC × GC solvation parameter model, the FAMEs elute beneath the hydrocarbons when the DB-210 × HP-50+ column set is employed. Unlike the chromatograms produced by previously published separations of biodiesel blends [9–12], the FAMEs occupy a unique region of the 2-D chromatogram and do not co-elute with the petroleum hydrocarbons. Increasing the unsaturation level of the C18 FAMEs increases the secondary retention. Although this decreases the separation between the FAMEs and hydrocarbons, all of the C18 FAMEs are still fully resolved from the hydrocarbons. The DB-210 × HP-50+ column set was not capable of fully separating the individual C18 FAMEs from one another. This is acceptable when the analytical goal is to determine total FAME content of a fuel (as would be the case for screening aviation fuel), but this would not be acceptable if the goal was to determine the amounts of the individual FAMEs.

Soybean biodiesel blends and coconut biodiesel blends were also analyzed with the GC × GC method. The soybean blend had a FAME distribution similar to that of the laboratory-prepared blend shown in Fig. 3, and the FAMEs were clearly separated from the hydrocarbons. However, the coconut blend had much higher levels of small saturated FAMEs including C8:0, C10:0, C12:0, and C14:0. While these FAMEs had decreased primary retention time, they eluted beneath the hydrocarbons in a manner similar to that seen in Fig. 3 for the C16:0 and C17:0 FAMEs. It is assumed that the low molecular weight FAMEs found in coconut biodiesel can be monitored in petroleum blends with the same efficacy as the C16, C17, and C18 FAMEs that were analyzed extensively in this study. Thus, the DB-210 × HP-50+ stationary phase pair is ideally suited for analyzing a wide range of FAMEs present in biodiesel blends.

4.2. GC × GC separation of kerosene containing low levels of FAMEs

A GC × GC chromatogram of pure kerosene is shown in Fig. 4A. The chromatogram shows a similar set of hydrocarbon peaks as the petroleum diesel except that the intensity of the hydrocarbon region diminishes rapidly at a primary retention time near 900 s whereas the diesel fuel hydrocarbons extend out to 1200 s. This difference is due to the lower boiling range of kerosene when compared to diesel fuel.

The signal axis in Fig. 4A is scaled from 8 pA to 1000 pA. This scale is reduced in Fig. 4B to a range from 8 pA to 28 pA. This increases the intensity of the signal axis by approximately a factor of 50. However, even under these display settings, there is unoccupied chromatographic space beneath the hydrocarbons. Fig. 4C shows a GC × GC chromatogram of kerosene spiked with a small quantity of the 1.0% biodiesel blend. In this case, the biodiesel blend was diluted with kerosene so that the individual FAMEs were present at 56 ppm. The FAMEs are separated from the hydrocarbons and the column bleed. This particular chromatogram is for a 100–1 split injection. When a 10–1 split injection was performed, the primary resolution of the most intense hydrocarbons was reduced presumably due to overloading of the primary stationary phase. However, the primary and secondary peak widths of the FAMEs were not changed

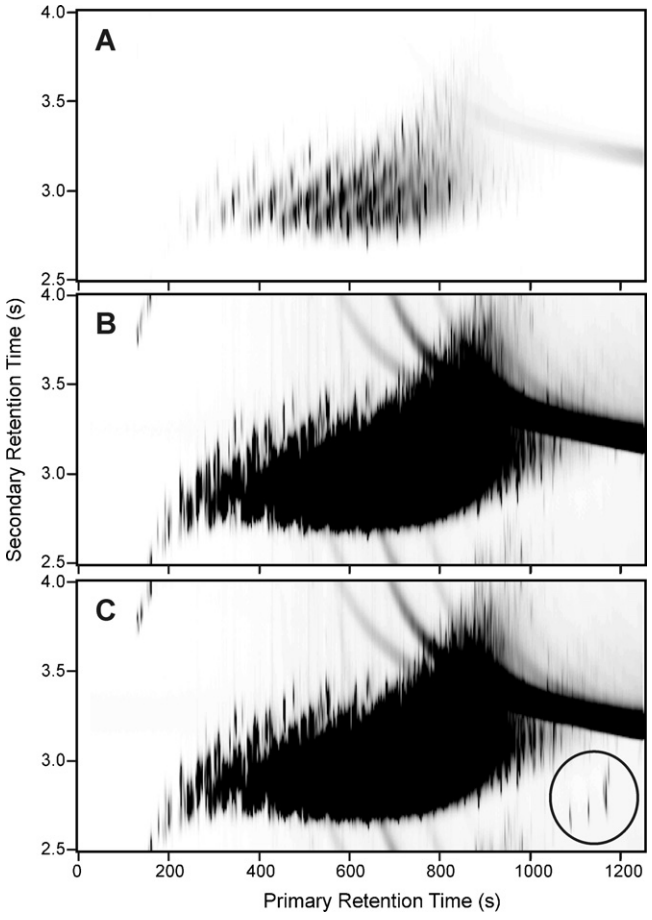

Fig. 4. GC × GC chromatograms of kerosene obtained with a 100–1 split injection: (A) pure kerosene with signal axis scaled from 8 to 100 pA; (B) pure kerosene with signal axis scaled from 8 to 28 pA; (C) kerosene containing 56 ppm of six different FAMEs with signal axis scaled from 8 to 28 pA.

by switching to a 10–1 split, and the peak areas were increased by a factor of 10.

Six samples were prepared with individual FAME concentrations of 2, 5, 11, 23, 56, and 98 ppm (w/w) by diluting the 1.0% biodiesel blend with varying amounts of kerosene. The samples were analyzed with a 10 to 1 split injection. The peak areas of the C16:0 and C17:0 FAMEs were determined individually, but the four C18 FAMEs were integrated as a group as they were not fully resolved from one another. The peak areas of the C16:0, C17:0, and C18 FAME peak areas were plotted as a function of concentration in ppm. In all three cases, highly linear plots were observed. Least square fits to the data generated the following regression parameters:

C16:0: slope = 0.512 ± 0.014; intercept = 0.07 ± 0.66; standard error = 1.2; $R^2 = 0.997$
C17:0: slope = 0.503 ± 0.008; intercept = 0.21 ± 0.37; standard error = 0.65; $R^2 = 0.999$
C18: slope = 0.503 ± 0.002; intercept = 0.09 ± 0.43; standard error = 0.77; $R^2 = 0.999$

Replicate analyses were performed for the 5 ppm and 2 ppm mixtures. The relative standard deviations for the FAME peak areas were 2% for the 5 ppm mixture and 7% for the 2 ppm mixture. Based on these results, it was concluded that individual FAME concentrations as low as 2 ppm can be detected and successfully quantified in petroleum-based fuels. It is probable that this limit could be reduced further by employing a splitless sample injection.

5. Conclusions

This study demonstrates how the GC × GC solvation parameter model can be used to identify promising pairs of stationary phases for isolating key compound classes from complex sample matrices. In the case of separating of FAMEs from petroleum-based fuel hydrocarbons, the model correctly predicts that the coupling of a fairly polar stationary phase, poly (methyltrifluoropropyl siloxane), with a semi-polar stationary phase, poly (dimethyldiphenylsiloxane) allows the FAMEs to be fully separated from the hydrocarbons on the secondary dimension. Such a stationary phase pair goes against the "conventional wisdom" that the best GC × GC separations are generated when polarity difference between the stationary phases is maximized. Instead, this study shows that it is better to choose stationary phases that best exploit the differences in the solubility characteristics of the analytes and the interferences. This model is a simple tool for identifying the solubility differences and matching them to an appropriate stationary phase pair. The GC × GC method developed in this study is effective at characterizing the concentration of individual FAMEs when their levels are as low as 2 ppm. This sensitivity should be more than adequate for determining if the total FAME content of jet fuel exceeds the 30 ppm limit set by the FAA [1].

Acknowledgment

This work was supported in part by a grant from the Agilent Foundation.

References

[1] U.S. Federal Aviation Administration, Special Airworthiness Information Bulletin: Jet Fuel Containing FAME (Fatty Acid Methyl Ester), NE-09-25R1, 2009.
[2] R.E. Pauls, J. Chromatogr. Sci. 49 (2011) 384.
[3] T.A. Foglia, K.C. Jones, J.G. Phillips, Chromatographia 62 (2005) 115.
[4] M. Kaminski, E. Gilgenast, A. Przyjazny, G. Romanik, J. Chromatogr. A 1122 (2006) 153.
[5] C. Ragonese, P.Q. Tranchida, D. Sciarrone, L. Mondello, J. Chromatogr. A 1216 (2009) 8992.
[6] D.D. Rocha, D.K. Barros, E.J.C. Costa, K.S. Souza, R.R. Passos, V.F. da Veiga, J.D. Chaar, Quim. Nova 31 (2008) 1062.
[7] C.M. Reddy, J.A. Demello, C.A. Carmichael, E.E. Peacock, L. Xu, J.S. Arey, Environ. Sci. Technol. 42 (2008) 2476.
[8] R.C.M. Faria, M.J.C. Rezende, C.M. Rezende, A.C. Pinto, Quim. Nova 30 (2007) 1900.
[9] J.V. Seeley, S.K. Seeley, E.K. Libby, J.D. McCurry, J. Chromatogr. Sci. 45 (2007) 650.
[10] F. Adam, F. Bertoncini, V. Coupard, N. Charon, D. Thiebaut, D. Espinat, M.C. Hennion, J. Chromatogr. A 1186 (2008) 236.
[11] W. Tiyapongpattana, P. Wilairat, P.J. Marriott, J. Sep. Sci. 31 (2008) 2640.
[12] K.M. Pierce, S.P. Schale, Talanta 83 (2011) 1254.
[13] J.V. Seeley, E.M. Libby, K.A.H. Edwards, S.K. Seeley, J. Chromatogr. A 1216 (2009) 1650.
[14] M.H. Abraham, A. Ibrahim, A.M. Zissimos, J. Chromatogr. A 1037 (2004) 29.
[15] C.F. Poole, S.K. Poole, J. Chromatogr. A 1184 (2008) 254.
[16] C.F. Poole, S.N. Atapattu, S.K. Poole, A.K. Bell, Anal. Chim. Acta 652 (2009) 32.
[17] J.A. Platts, D. Butina, M.H. Abraham, A. Hersey, J. Chem. Inf. Comput. Sci. 39 (1999) 835.
[18] S.N. Atapattu, K. Eggers, C.F. Poole, W. Kiridena, W.W. Koziol, J. Chromatogr. A 1216 (2009) 1640.
[19] S.N. Atapattu, C.F. Poole, J. Chromatogr. A 1195 (2008) 136.
[20] J.V. Seeley, N.J. Micyus, J.D. McCurry, S.K. Seeley, Am. Lab. 38 (2006) 24.